AAS 22-725

MODULAR DYNAMIC MODELING OF HINGED SOLAR PANEL DEPLOYMENTS

Galen Bascom* **and Hanspeter Schaub†**

Prior multi-body dynamics work using the back-substitution method is expanded to apply to deployable spacecraft panel configurations. Earlier work focused on studying first order flexing of solar panels about a fixed angle. This study models deployable structures which are allowed to flex about a nominal, time-varying deployment angle. External motor torques are included in the dynamical formulation to create a physics-based deployable panel simulation. The full nonlinear coupling is retained while providing an implementable, modular software solution using the back-substitution method. The Basilisk simulation framework is used to illustrate the implementation, with numerical results are shown for both nominal and off-nominal deployments.

INTRODUCTION

While the problem of modeling solar array deployment has garnered research interest for a long time, the need for implementable software solutions has been highlighted.[1] Fully representing a spacecraft with deployable solar panels as a rigid body with flexible appendages requires a set of unwieldy, coupled non-linear equations. Certain simplifying approaches, such as assuming that the coupling with the translational motion is negligible or limiting the effect to a single plane of motion, compromise the underlying dynamics. Such assumptions make the problem more analytically tractable but may be insufficiently general or degrade performance unacceptably.

An implementable model for simulating a deployable solar panel about a single fixed hinge is introduced here. While solar arrays come in many different configurations, this model covers a range of useful cases and serves as a starting point for further analysis. In addition to studying nominal cases, this work also demonstrates one way of modeling off-nominal deployments. Many recorded spacecraft anomalies are because of deployment faults or failures,[2] making these capabilities useful.

Expanding on previous work on deployable hinged panels, a back-substitution method is used to make the simulation both fast and modular.[3,4] Making the often-satisfied assumption that each component of the spacecraft is attached to a rigid hub yields a system mass matrix that, while not diagonal, has a predictable structure where the coupling between variables happens through the hub. The method exploits that structure, solving first for the spacecraft rigid-body translational and rotational accelerations, and then substituting those values back in to solve for the other second-order state derivatives.

*PhD Student, Ann and H.J. Smead Department of Aerospace Engineering Sciences, University of Colorado, Boulder, Boulder, CO, 80309. AAS Member.

†Professor and Department Chair, Schaden Leadership Chair, Ann and H.J. Smead Department of Aerospace Engineering Sciences, University of Colorado, Boulder, 431 UCB, Colorado Center for Astrodynamics Research, Boulder, CO, 80309. AAS Fellow, AIAA Fellow.

The novelty in this work is that it does not assume a fixed reference angle but instead introduces a time-varying reference, which allows for a wider range of scenarios including deployments demonstrating both nominal and off-nominal behavior. A deployment profiler, panel angle sensor, and panel motor are added to facilitate modeling deployment scenarios. Moreover, due to the modular structure of the proposed software implementation, it is straightforward to add other features, for example the solar panel power. This makes it possible to simulate complex, linked behaviors with relative ease. This paper uses the proposed solution as implemented in the Basilisk software architecture for both nominal and off-nominal deployments, and the resulting numerical results are presented.

PROBLEM STATEMENT

In order to develop the equations of motion to integrate, the relevant coordinate frames are first defined as seen in Figure 1. The description is general, allowing for the panel to be placed in any configuration relative to the spacecraft, and it easily extended to multiple panels. The assumption is that the spacecraft hub as well as the panels individually are rigid and connected by hinge with a single degree of freedom. The hinge is modeled as a spring with torsional stiffness coefficient k and viscous damping coefficient c.

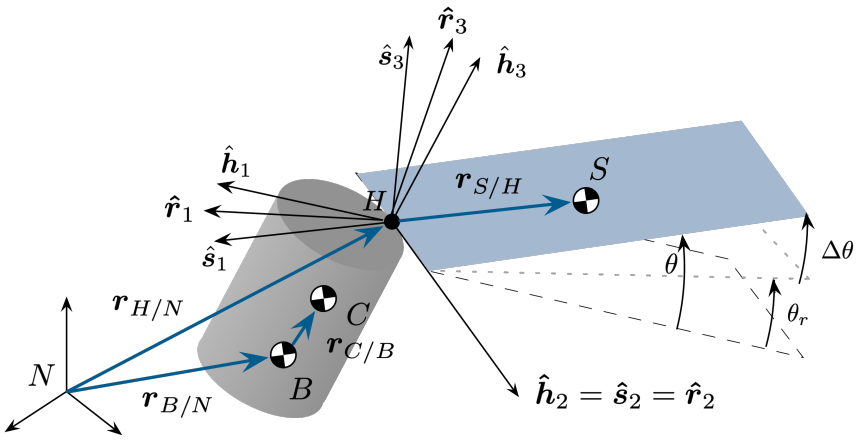

Figure 1. Reference frame definitions for deployable hinged panel problem.

The relevant coordinate frames are as follows. The inertial reference frame is $\mathcal{N}$:$\{\hat{\boldsymbol{n}}_1, \hat{\boldsymbol{n}}_2, \hat{\boldsymbol{n}}_3\}$ with an origin at point N. The body (hub) fixed frame is $\mathcal{B}$:$\{\hat{\boldsymbol{b}}_1, \hat{\boldsymbol{b}}_2, \hat{\boldsymbol{b}}_3\}$ with an origin at body-fixed point B. Although it is sometimes convenient to also define a separate point for the body-fixed hub center of mass, the simplifying assumption is made that the center of mass of the hub is coincident with point B. The hinge frame, with its origin at the hinge point H, is $\mathcal{H}$:$\{\hat{\boldsymbol{h}}_1, \hat{\boldsymbol{h}}_2, \hat{\boldsymbol{h}}_3\}$. The hinge frame is fixed relative to the body.

The panel frame $\mathcal{S}$:$\{\hat{\boldsymbol{s}}_1, \hat{\boldsymbol{s}}_2, \hat{\boldsymbol{s}}_3\}$ has its origin at point H, and the panel center of mass S lies along $\hat{\boldsymbol{s}}_1$ such that $\boldsymbol{r}_{S/H} = -d\hat{\boldsymbol{s}}_1$, where d is a fixed distance. The panel unit vector $\hat{\boldsymbol{s}}_2$ is defined so that the rotation angle θ about the $\hat{\boldsymbol{s}}_2$ axis relative to the fixed hinge frame is positive by the right-hand

rule. Finally, $\hat{\boldsymbol{s}}_3$ completes the right-handed set. The $\mathcal{S}$ frame is assumed to yield a diagonal inertia mass matrix for the panel.

The last frame is the reference frame $\mathcal{R}$:$\{\hat{\boldsymbol{r}}_1, \hat{\boldsymbol{r}}_2, \hat{\boldsymbol{r}}_3\}$, again with its origin at H. Just as $\mathcal{S}$ differs from $\mathcal{H}$ by a rotation θ along $\hat{\boldsymbol{h}}_2$, $\mathcal{R}$ differs from $\mathcal{H}$ by a rotation along $\hat{\boldsymbol{h}}_2$, this time by an angle θ_r. For a deployed structure, θ_r would be fixed, but during deployment or other articulation it would be time-varying. The introduction of this new coordinate frame adds the new quantity $\Delta\theta = \theta - \theta_r$. The hinge stiffness and viscous friction are defined not relative to θ, as in prior work, but instead relative to $\Delta\theta$.

DERIVATION OF EQUATIONS OF MOTION

The equations of motion are defined using a back-substitution method previously described by Allard and Schaub.[4,5] For a more complete derivation, those prior works should be referenced. The salient equations and steps are shown here, with differences identified. The translational and rotational equations, as well as the equations for the solar panel motion, are derived using Newtonian and Eulerian methods. As for notation, the inertial derivative of a vector $\boldsymbol{v}$ is $\dot{\boldsymbol{v}}$, while the body-frame derivative is denoted $\boldsymbol{v'}$. The cross-product equivalent matrix is denoted $[\tilde{\boldsymbol{v}}]$.

Translational Equations of Motion

The center of mass of the spacecraft, by Newton's second law, follows

$$\boldsymbol{F}_{\text{ext}} = m_{\text{sc}}\ddot{\boldsymbol{r}}_{C/N} \tag{1}$$

where $\boldsymbol{F}_{\text{ext}}$ is the sum of the external forces acting on the system, m_{sc} is the total spacecraft mass, and $\boldsymbol{r}_{C/N}$ is the position vector of the spacecraft center of mass point C relative to N. Similar notation is used for other position, velocity, and acceleration vectors. The translational equations of motion reduce to the equation:

$$\begin{gathered} m_{\text{sc}}\ddot{\boldsymbol{r}}_{B/N} - m_{\text{sc}}\boldsymbol{r}_{C/B} \times \dot{\boldsymbol{\omega}}_{\mathcal{B}/\mathcal{N}} + m_{\text{sp}} d\hat{\boldsymbol{s}}_3\ddot{\theta} = \\ \boldsymbol{F}_{\text{ext}} - 2m_{\text{sc}}\boldsymbol{\omega}_{\mathcal{B}/\mathcal{N}} \times \boldsymbol{r}'_{C/B} - m_{\text{sc}}\boldsymbol{\omega}_{\mathcal{B}/\mathcal{N}} \times (\boldsymbol{\omega}_{\mathcal{B}/\mathcal{N}} \times \boldsymbol{r}_{C/B}) - m_{\text{sp}} d\dot{\theta}^2\hat{\boldsymbol{s}}_1 \end{gathered} \tag{2}$$

The angular velocity vector of frame $\mathcal{B}$ relative to frame $\mathcal{N}$ is $\boldsymbol{\omega}_{\mathcal{B}/\mathcal{N}}$.

Rotational Equations of Motion

The starting point for deriving the rotational equations of motion is Euler's equation:

$$\dot{\boldsymbol{H}}_{\text{sc},B} = \boldsymbol{L}_B + m_{\text{sc}}\ddot{\boldsymbol{r}}_{B/N} \times \boldsymbol{r}_{C/B} \tag{3}$$

The relevant quantities are $\dot{\boldsymbol{H}}_{\text{sc},B}$, the inertial derivative of the angular momentum of the spacecraft, as well as $\boldsymbol{L}_B$, the torque about point B. The final term is included because point B is not coincident with C. The angular momentum of the spacecraft about B is:

$$\boldsymbol{H}_{\text{sc},B} = [I_{\text{hub},B}]\boldsymbol{\omega}_{\mathcal{B}/\mathcal{N}} + [I_{\text{sp},S}]\boldsymbol{\omega}_{\mathcal{B}/\mathcal{N}} + \dot{\theta} I_{S_2}\hat{\boldsymbol{s}}_2 + m_{\text{sp}}\boldsymbol{r}_{S/B} \times \dot{\boldsymbol{r}}_{S/B} \tag{4}$$

The quantity $[I_{\text{hub},B}]$ is the moment of inertia of the hub about point B. Likewise $[I_{\text{sp},S}]$ is the moment of inertia of the panel about point S, and I_{S_2} is the inertia of the panel about S (corresponding

to a rotation about $\hat{\boldsymbol{s}}_2$) from the diagonal inertia matrix. The inertial time derivative is evaluated and relevant substitutions made to yield the form:

$$\begin{aligned} m_{\text{sc}}\boldsymbol{r}_{C/B} \times \ddot{\boldsymbol{r}}_{B/N} + [I_{\text{sc},B}]\dot{\boldsymbol{\omega}}_{\mathcal{B}/\mathcal{N}} + (I_{S_2}\hat{\boldsymbol{s}}_2 + m_{\text{sp}}d\boldsymbol{r}_{S/B} \times \hat{\boldsymbol{s}}_3)\ddot{\theta} = -\boldsymbol{\omega}_{\mathcal{B}/\mathcal{N}} \times [I_{\text{sc},B}]\boldsymbol{\omega}_{\mathcal{B}/\mathcal{N}} - \\ [I'_{\text{sc},B}]\boldsymbol{\omega}_{\mathcal{B}/\mathcal{N}} - \dot{\theta}\boldsymbol{\omega}_{\mathcal{B}/\mathcal{N}} \times (I_{S_2}\hat{\boldsymbol{s}}_2 + m_{\text{sp}}d\boldsymbol{r}_{S/B} \times \hat{\boldsymbol{s}}_3) + m_{\text{sp}}d\dot{\theta}^2\boldsymbol{r}_{S/B} \times \hat{\boldsymbol{s}}_1 + \boldsymbol{L}_B \end{aligned} \tag{5}$$

The quantity $[I_{\text{sc},B}]$ is the moment of inertia of the full spacecraft about point B.

Panel Equation of Motion

The torque $\boldsymbol{L}_H$ acting on the panel about point H can be defined as:

$$\boldsymbol{L}_H = L_{H_1}\hat{\boldsymbol{s}}_1 + L_{H_2}\hat{\boldsymbol{s}}_2 + L_{H_3}\hat{\boldsymbol{s}}_3 = L_{H_2}\hat{\boldsymbol{s}}_2 \tag{6}$$

The component torques L_1 and L_3 are ignored for these purposes, as the only degree of freedom is rotation about $\hat{\boldsymbol{s}}_2$. The remaining torque can be written as

$$L_{H_2} = -k\Delta\theta - c\Delta\dot{\theta} + u \tag{7}$$

where u is the motor torque acting on the panel. This is a departure from previous work,[5] where the equation was relative only to θ.

The inertial angular velocity of the panel is

$$\boldsymbol{\omega}_{\mathcal{S}/\mathcal{N}} = \boldsymbol{\omega}_{\mathcal{S}/\mathcal{B}} + \boldsymbol{\omega}_{\mathcal{B}/\mathcal{N}} = \dot{\theta}\hat{\boldsymbol{s}}_2 + \omega_{S_1}\hat{\boldsymbol{s}}_1 + \omega_{S_2}\hat{\boldsymbol{s}}_2 + \omega_{S_3}\hat{\boldsymbol{s}}_3 \tag{8}$$

where the last three terms are defined to be the components of $\boldsymbol{\omega}_{\mathcal{B}/\mathcal{N}}$ in the $\mathcal{S}$ frame.

The relevant Euler equation of motion is:

$$I_{S_2}(\dot{\omega}_{S_2} + \ddot{\theta}) = -(I_{S_1} - I_{S_3})\omega_{S_1}\omega_{S_3} + L_{S_2} \tag{9}$$

with $\boldsymbol{L}_S = L_{S_1}\hat{\boldsymbol{s}}_1 + L_{S_2}\hat{\boldsymbol{s}}_2 + L_{S_3}\hat{\boldsymbol{s}}_3$ the torque on the panel about its center of mass, I_{S_i} the panel moments of inertia about the three corresponding principal axes.

To find L_{S_2}, note that

$$\boldsymbol{L}_S = \boldsymbol{L}_H - \boldsymbol{r}_{S/H} \times m_{\text{sp}}\ddot{\boldsymbol{r}}_{S/N} = \boldsymbol{L}_H + d\hat{\boldsymbol{s}}_1 \times m_{\text{sp}}\ddot{\boldsymbol{r}}_{S/N} \tag{10}$$

Following again the derivation in prior work,[5] with the notable difference that the hinge stiffness and viscous damping are computed relative to the reference angle, the final panel equation of motion is:

$$\begin{aligned} \ddot{\theta} = (I_{S_2} + m_{\text{sp}}d^2)^{-1}(-m_{\text{sp}}d\hat{\boldsymbol{s}}_2^T\ddot{\boldsymbol{r}}_{B/N} - [(I_{S_2} + m_{\text{sp}}d^2)\hat{\boldsymbol{s}}_2^T - m_{\text{sp}}d\hat{\boldsymbol{s}}_3^T][\tilde{\boldsymbol{r}}_{H/B}]\dot{\boldsymbol{\omega}}_{\mathcal{B}/\mathcal{N}} \\ -k\Delta\theta - c\Delta\dot{\theta} + u + (I_{S_3} - I_{S_1} + m_{\text{sp}}d^2)\omega_{S_1}\omega_{S_3} - m_{\text{sp}}d\hat{\boldsymbol{s}}_3^T[\tilde{\boldsymbol{\omega}}_{\mathcal{B}/\mathcal{N}}][\tilde{\boldsymbol{\omega}}_{\mathcal{B}/\mathcal{N}}]\boldsymbol{r}_{H/B}) \end{aligned} \tag{11}$$

While it might be expected to see $\Delta\ddot{\theta}$ in the final equation, the hinge torque depends only on the angular position and velocity, so those are the only quantities for which the introduction of the reference angle and the redefinition of the hinge model make a difference.

Backsubstitution Method

The panel equation of motion can be simplified to the form

$$\ddot{\theta} = \boldsymbol{a}_\theta^T \ddot{\boldsymbol{r}}_{B/N} + \boldsymbol{b}_\theta^T \dot{\boldsymbol{\omega}}_{\mathcal{B}/\mathcal{N}} + c_\theta \tag{12}$$

by defining the corresponding quantities:

$$\boldsymbol{a}_\theta = -\frac{m_{\text{sp}} d}{I_{S_2} + m_{\text{sp}} d^2} \hat{\boldsymbol{s}}_3 \tag{13}$$

$$\boldsymbol{b}_\theta = -\frac{1}{I_{S_2} + m_{\text{sp}} d^2} [(I_{S_2} + m_{\text{sp}} d^2) \hat{\boldsymbol{s}}_2 + m_{\text{sp}} d [\tilde{\boldsymbol{r}}_{H/B}] \hat{\boldsymbol{s}}_3] \tag{14}$$

$$c_\theta = \frac{1}{I_{S_2} + m_{\text{sp}} d^2} (-k\Delta\theta - c\Delta\dot{\theta} + u + (I_{S_3} - I_{S_1} + m_{\text{sp}} d^2)\omega_{S_1}\omega_{S_3} - m_{\text{sp}} d \hat{\boldsymbol{s}}_3^T [\tilde{\boldsymbol{\omega}}_{\mathcal{B}/\mathcal{N}}][\tilde{\boldsymbol{\omega}}_{\mathcal{B}/\mathcal{N}}] \boldsymbol{r}_{H/B}) \tag{15}$$

By making the appropriate substitutions into Eqs. (2) and (5), the coupled translational and rotational hub equations of motion can be written in the form:

$$\begin{bmatrix} [A] & [B] \\ [C] & [D] \end{bmatrix} \begin{bmatrix} \ddot{\boldsymbol{r}}_{B/N} \\ \dot{\boldsymbol{\omega}}_{\mathcal{B}/\mathcal{N}} \end{bmatrix} = \begin{bmatrix} \boldsymbol{v}_{\text{t}} \\ \boldsymbol{v}_{\text{r}} \end{bmatrix} \tag{16}$$

To generate this compact, tractable form, newly defined variables are:

$$[A] = m_{\text{sc}} [I_{3\times 3}] + m_{\text{sp}} d \hat{\boldsymbol{s}}_3 \boldsymbol{a}_\theta^T \tag{17}$$

$$[B] = -m_{\text{sc}} [\tilde{\boldsymbol{r}}_{C/B}] + m_{\text{sp}} d \hat{\boldsymbol{s}}_3 \boldsymbol{b}_\theta^T \tag{18}$$

$$[C] = m_{\text{sc}} [\tilde{\boldsymbol{r}}_{C/B}] + (I_{S_2} \hat{\boldsymbol{s}}_2 + m_{\text{sp}} d [\tilde{\boldsymbol{r}}_{S/B}] \hat{\boldsymbol{s}}_3) \boldsymbol{a}_\theta^T \tag{19}$$

$$[D] = [I_{\text{sc},B}] + (I_{S_2} \hat{\boldsymbol{s}}_2 + m_{\text{sp}} d [\tilde{\boldsymbol{r}}_{S/B}] \hat{\boldsymbol{s}}_3) \boldsymbol{b}_\theta^T \tag{20}$$

$$\boldsymbol{v}_{\text{t}} = \boldsymbol{F}_{\text{ext}} - 2m_{\text{sc}} \boldsymbol{\omega}_{\mathcal{B}/\mathcal{N}} \times \boldsymbol{r}'_{C/B} - m_{\text{sc}} \boldsymbol{\omega}_{\mathcal{B}/\mathcal{N}} \times (\boldsymbol{\omega}_{\mathcal{B}/\mathcal{N}} \times \boldsymbol{r}_{C/B}) - (m_{\text{sp}} d \dot{\theta}^2 \hat{\boldsymbol{s}}_1 + m_{\text{sp}} d c_\theta \hat{\boldsymbol{s}}_3) \tag{21}$$

$$\begin{aligned} \boldsymbol{v}_{\text{r}} = &-(\dot{\theta}[\tilde{\boldsymbol{\omega}}_{\mathcal{B}/\mathcal{N}}] + c_\theta [I_{3\times 3}])(I_{S_2} \hat{\boldsymbol{s}}_2 + m_{\text{sp}} d \boldsymbol{r}_{S/B} \times \hat{\boldsymbol{s}}_3) + m_{\text{sp}} d \dot{\theta}^2 \boldsymbol{r}_{S/B} \times \hat{\boldsymbol{s}}_1 \\ &-\boldsymbol{\omega}_{\mathcal{B}/\mathcal{N}} \times [I_{\text{sc},B}] \boldsymbol{\omega}_{\mathcal{B}/\mathcal{N}} - [I'_{\text{sc},B}] \boldsymbol{\omega}_{\mathcal{B}/\mathcal{N}} + \boldsymbol{L}_B \end{aligned} \tag{22}$$

Using the Schur complement of the partitioned matrix, solving this system of linear equations is a matter of solving:

$$\dot{\boldsymbol{\omega}}_{\mathcal{B}/\mathcal{N}} = ([D] - [C][A]^{-1}[B])^{-1} (\boldsymbol{v}_{\text{r}} - [C][A]^{-1} \boldsymbol{v}_{\text{t}}) \tag{23}$$

$$\ddot{\boldsymbol{r}}_{B/N} = [A]^{-1} (\boldsymbol{v}_{\text{t}} - [B] \dot{\boldsymbol{\omega}}_{\mathcal{B}/\mathcal{N}}) \tag{24}$$

Finally, these results are in turn substituted back in to the Eq. (12) to solve for $\ddot{\theta}$. This method has been shown to be a computationally efficient way of simulating complex multibody systems.[4] The modest changes to the hinged spring model expand this useful framework to permit deployment angles with a time-varying reference.

SOFTWARE IMPLEMENTATION

Many approaches could be used to simulate the dynamics represented by the above equations of motion. The selected method is by no means the only way, but it does represent a convenient one. Basilisk is a flight-proven software architecture that uses the back-substitution method to achieve good computational performance while retaining high fidelity.[3] The back-substitution method lends itself to a modular approach, where the spacecraft and simulation are assembled from a wide range of components such reaction wheels, fuel tanks, and sensors. This enables customizable and scalable dynamical modeling of intricate systems. The complex dynamics do not need to be rederived each time, as each individual set of state variables (for example the θ and $\dot{\theta}$ from a hinged panel) that affect the dynamics can be isolated to determine that object's individual contributions to the $[A]$, $[B]$, $[C]$, and $[D]$ matrices. Similar work demonstrates these methods as applied to reaction wheels with jitter and fuel slosh.[6,7]

This software architecture was modified not only to reflect the changed dynamics due to the introduced reference angle, but also to permit practical deployments using those reference angles. A hinge angle sensor, deployment profiler, and hinge motor were added. The sensor incorporates simple Gaussian noise based on defined parameters. The deployment profiler permits a simple linear deployment. The user sets the angle and time for the start and end of deployment, and the profiler adjusts the reference frame linearly within that time frame. In the future, a more complicated profiler—for example, one that outputs a smoother profile—could be developed.

Finally, the hinge motor implements a control law to update the torque u on the panel. The control law used is:

$$u = -K\Delta\theta - P\Delta\dot{\theta} \tag{25}$$

The variable K is the proportional gain, while P is the derivative gain. A proportional-derivative type control law was chosen for convenience without a detailed analysis of its properties. It may be possible to improve upon this control law depending on the desired characteristics of the hinge motor. As it stands, this motor essentially has the effect of amplifying the natural dynamics of the hinge, as can be seen by substituting it in to Eq. (7).

Another advantage of the Basilisk implementation is that, because the panel object outputs its full state, including its position and attitude relative to the inertial frame, it is a simple matter of connecting that state message to other modules to allow components such as solar power modules and coarse sun sensors to attach to the panel and be affected by its dynamics. For example, a simple setup might include the following lines:

```
from Basilisk.simulation import hingedRigidBodyStateEffector
from Basilisk.simulation import simpleSolarPanel

# create panel structure
panel = hingedRigidBodyStateEffector.HingedRigidBodyStateEffector()

# create solar cells
solarPanel = simpleSolarPanel.SimpleSolarPanel()

# subscribe messages
solarPanel.stateInMsg.subscribeTo(panel.hingedRigidBodyConfigLogOutMsg)
solarPanel.sunInMsg.subscribeTo(sunStateMsg)
```

Other aspects of the code, including setting the parameters and creating the sun state message, are omitted for brevity. Nonetheless, this short example demonstrates the ease of scripting a nontrivial simulation with complex, layered behaviors.

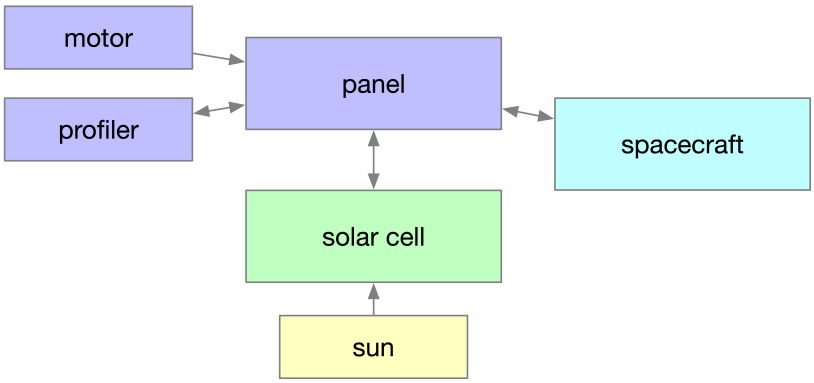

Figure 2. Simulation modules for panel deployment demonstration.

Figure 2 diagrams the Basilisk modules used in the simulation scenario. Each block is a module, and the arrows represent messaging pathways.

SIMULATION RESULTS

The simulation involved a spacecraft pointing at the sun from a distance of 1 AU. The initial attitude was set to the inertial frame attitude with a zero initial body rate. A panel attached to the rigid hub (with a hinge frame aligned with the body frame) was deployed. No noise was added to the panel sensor and instead the panel state was passed directly to the motor module. The simulation first demonstrates a full deployment from $\theta_r = -\pi/2$ to $\theta_r = 0$, and it also shows where the panel gets stuck at $\theta_r = -\pi/4$ (the off-nominal deployment). This was implemented simply by changing the profiler values correspondingly, while other types of deployment anomaly might be implemented differently. The solar panel power module connected to the module also shows the difference in power output.

Parameters for the individual modules were chosen to demonstrate the operation of the modules without necessarily being designed to be realistic. Those parameters are summarized in Table 1.

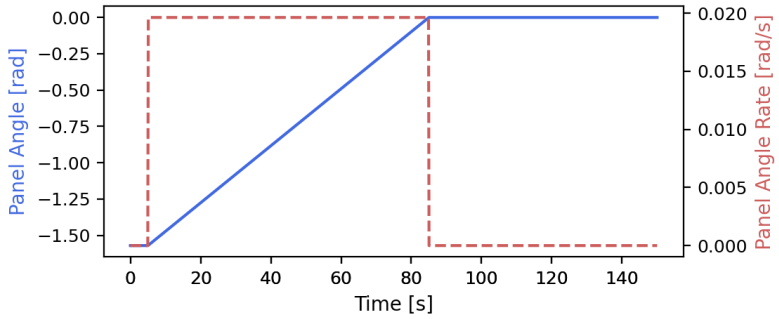

Figure 3. Reference panel angle and angle rate versus time for the nominal case.

Table 1. Parameters used in solar panel deployment simulation.

Parameter	Value	Units
Simulation time step	0.01	s
Spacecraft hub mass m_{hub}	750.0	kg
Spacecraft hub inertia $[I_{\text{hub},B}]$	$\begin{bmatrix} 900.0 & 0.0 & 0.0 \\ 0.0 & 800.0 & 0.0 \\ 0.0 & 0.0 & 600.0 \end{bmatrix}$	$kg \cdot m^2$
Panel mass m_{sp}	100.0	kg
Panel inertia $[I_{\text{sp},S}]$	$\begin{bmatrix} 100.0 & 0.0 & 0.0 \\ 0.0 & 50.0 & 0.0 \\ 0.0 & 0.0 & 50.0 \end{bmatrix}$	$kg \cdot m^2$
Panel distance to center of mass d	1.5	m
Panel torsional stiffness coefficient k	200.0	$N \cdot m/rad$
Panel viscous damping coefficient c	20.0	$N \cdot m \cdot s/rad$
Panel initial angle	$-\pi/2$	rad
Profiler start time	5.0	s
Profiler end time	85.0 (nom) 45.0 (off-nom)	s
Profiler start θ_r	$-\pi/2$	rad
Profiler end θ_r	0.0 (nom) $-\pi/4$ (off-nom)	rad
Motor proportional gain K	100.0	$N \cdot m/rad$
Motor derivative gain P	10.0	$N \cdot m \cdot s/rad$
Solar cell normal direction	$[0.0 \quad 0.0 \quad 1.0]$	
Solar cell area	2.0	m^2
Solar cell efficiency	0.9	

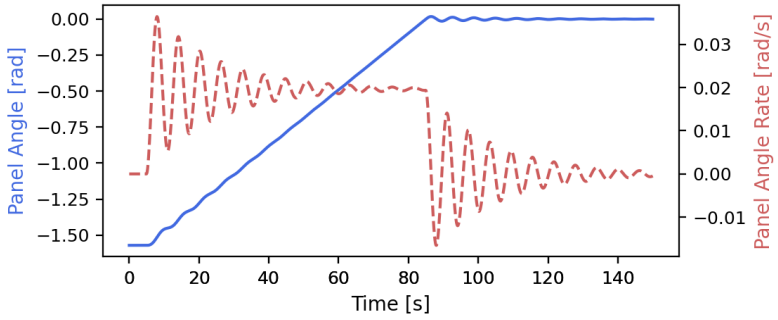

Figure 4. Actual panel angle and angle rate versus time for nominal case.

For the nominal case, the linear profile is as expected, with the panel deployment starting at $t = 5s$ and ending at $t = 85s$. The reference angle varies linearly between $\pi/2$ and 0 over that stretch, and it remains 0 afterwards. The actual panel angle naturally does not follow this profile perfectly. Due to the panel dynamics, oscillations appear about the varying reference angle.

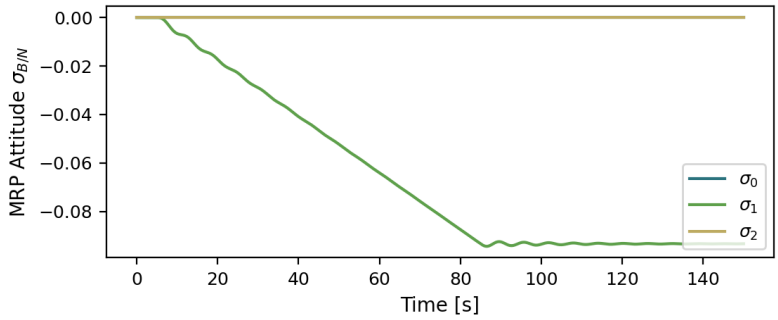

Figure 5. Attitude in MRPs versus time for the nominal case.

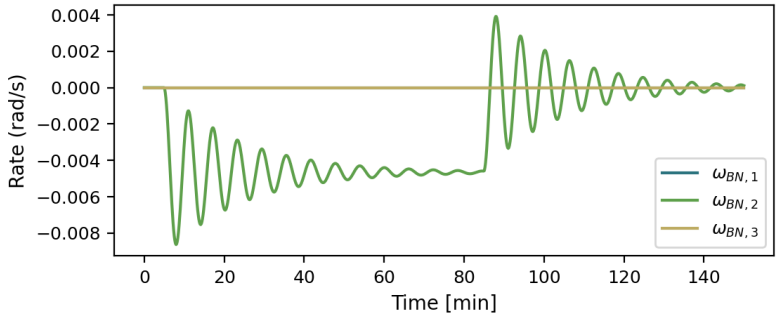

Figure 6. Body-frame body rates $\omega_{\mathcal{B}/\mathcal{N}}$ versus time for the nominal case.

The body frame rate and attitude show the coupled effect of the solar panel deployment on the hub attitude. As the panel deploys, a corresponding body rate modestly changes the angle of the reference frame $\mathcal{B}$. The attitude is presented in terms of modified Rodrigues parameters (MRPs).

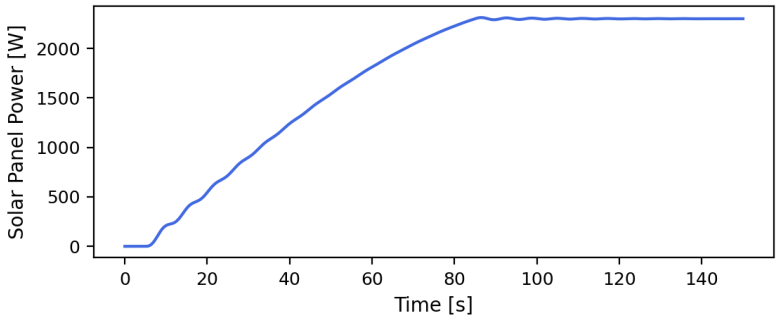

Figure 7. Solar panel power versus time for the nominal case.

As the solar panel power plot shows, the decreasing angle between the solar panel unit normal and the vector pointing from the spacecraft towards the sun also increases the power generated by the solar panel, as affected by the panel oscillations. This is as expected, and it reveals the usefulness of simply linking in the structural panel state message in order to provide the same motion to the

power generation module.

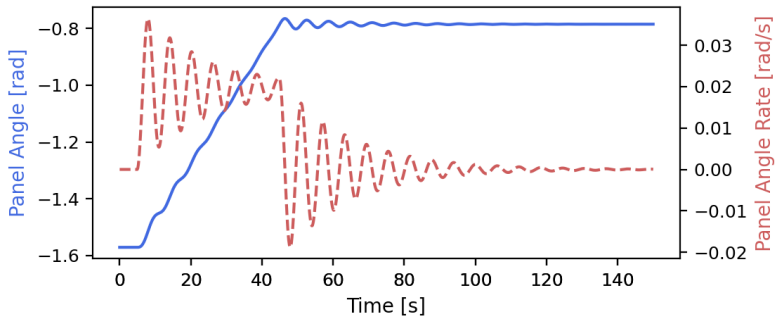

Figure 8. Actual panel angle and angle rate versus time for the off-nominal case.

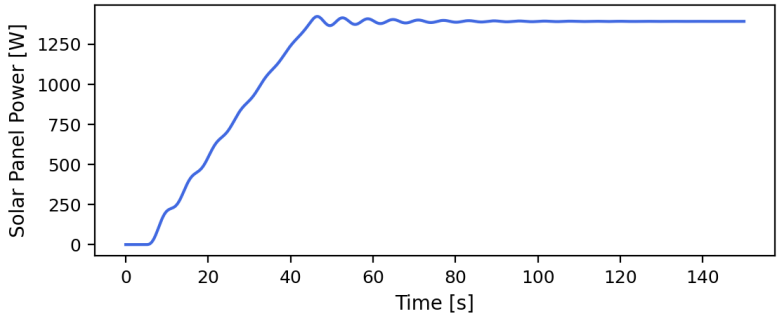

Figure 9. Solar panel power versus time for the off-nominal case.

For the off-nominal case, where the deployment gets "stuck" halfway through, the oscillations are still present but with a shorter deployment time, The final panel angle is lower, and the final power output is also significantly reduced.

In order to verify correct operation of the simulation, it is useful to evaluate the orbital and rotational angular momenta and energies. Those quantities are presented for the nominal deployment case.

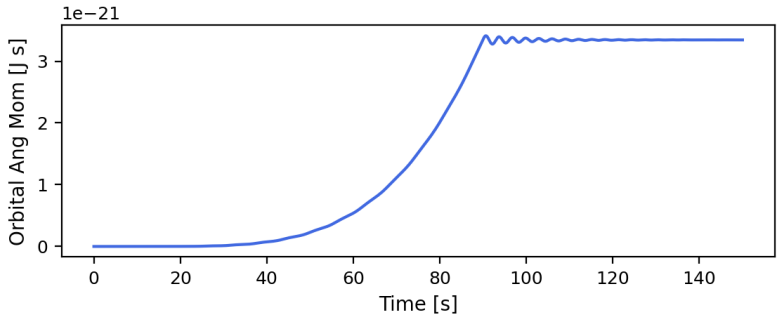

Figure 10. Magnitude of the orbital angular momentum versus time.

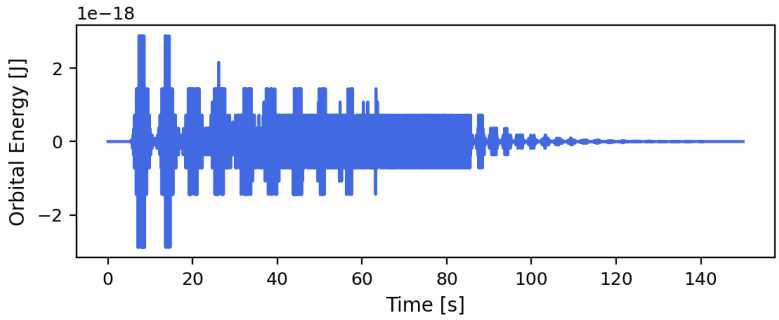

Figure 11. Orbital energy versus time.

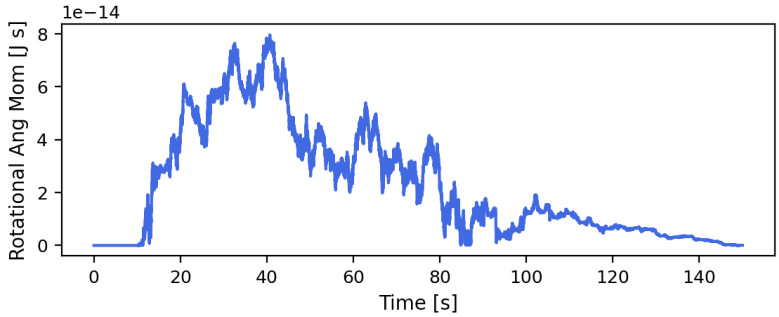

Figure 12. Magnitude of the rotational angular momentum versus time.

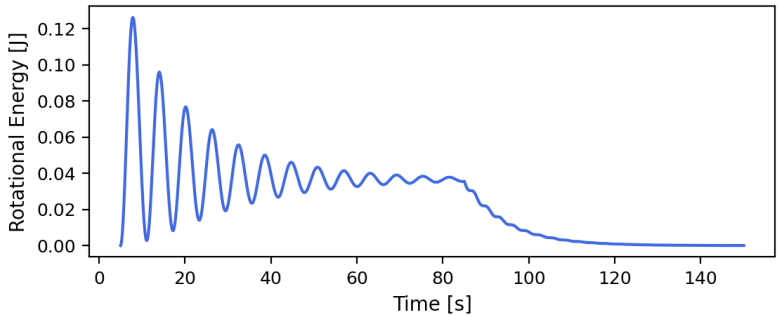

Figure 13. Rotational energy versus time.

The orbital energy and angular momentum are effectively untouched by the deployment of the panel. Similarly, the rotational angular momentum is effectively negligible. Because the torque is internal, it is expected that the rotational angular momentum should stay zero. In contrast, the rotational energy is not expected to be conserved throughout the motion. A system at rest that begins deploying its panels has nonzero rotational energy, with contributions coming from the moving panel, the moving hub, and the potential energy term $k(\Delta\theta)^2$.

CONCLUSION

This work extends previous work on hinged rigid panels attached to a rigid hub to permit deployments. While many different implementations are possible, the chosen implementation is flexible and modular, permitting a wide array of configurations that can be easily assembled from the components. The numerical simulations show the oscillations have changed to be around the reference angle over the course of a deployment, and the off-nominal deployment is shown to have a reduced power output. Future work will improve upon the simple profiler and motor modules as well as considering more complex deployable structures beyond rigid panels with a single hinge.

ACKNOWLEDGMENT

This work was supported by an Air Force STTR award No. 1154-00076 in collaboration with Verus Research.

REFERENCES

[1] B. Wie, N. Furumoto, A. K. Banerjee, and P. M. Barba, "Modeling and Simulation of Spacecraft Solar Array Deployment," *Journal of Guidance, Control, and Dynamics*, Vol. 9, No. 5, 1986, pp. 670–683.

[2] A. Rivera and A. Stewart, "Study of Spacecraft Deployables Failures," *European Space Mechanisms and Tribology Symposium*, Online, Sept. 20–24 2021.

[3] C. Allard, M. D. Ramos, H. Schaub, P. Kenneally, and S. Piggott, "Modular Software Architecture for Fully Coupled Spacecraft Simulations," *Journal of Aerospace Information Systems*, Vol. 15, No. 12, 2018, pp. 670–683.

[4] C. Allard, M. D. Ramos, and H. Schaub, "Computational Performance of Complex Spacecraft Simulations Using Back-Substitution," *Journal of Aerospace Information Systems*, Vol. 16, No. 10, 2019, pp. 427–436.

[5] C. Allard, H. Schaub, and S. Piggott, "General Hinged Rigid-Body Dynamics Approximating First-Order Spacecraft Solar Panel Flexing," *Journal of Spacecraft and Rockets*, Vol. 55, No. 5, 2018, pp. 1290–1298.

[6] J. Alcorn, C. Allard, and H. Schaub, "Fully Coupled Reaction Wheel Static and Dynamic Imbalance for Spacecraft Jitter Modeling," *AIAA Journal of Guidance, Control, and Dynamics*, Vol. 41, No. 6, 2018, pp. 1380–1388, 10.2514/1.G003277.

[7] C. Allard, M. Diaz-Ramos, and H. Schaub, "Spacecraft Dynamics Integrating Hinged Solar Panels and Lumped-Mass Fuel Slosh Model," *AIAA/AAS Astrodynamics Specialist Conference*, Long Beach, CA, Sept. 12–15 2016.